

## Spatial inhomogeneity and void-growth kinetics in the decomposition of ultrathin oxide overlayers on Si(100)

Y.-K. Sun, D. J. Bonser, and Thomas Engel

*Department of Chemistry BG-10, University of Washington, Seattle, Washington 98195*

(Received 30 November 1990)

Oxide layers whose thickness is 4–10 monolayers decompose inhomogeneously through void formation in which the clean surface is exposed. No changes take place in the oxide region during thermal desorption until it is engulfed by the growing voids. The kinetics of void formation has been measured with isothermal and temperature-programmed methods. A strong similarity to kinetic parameters determined for high-temperature reactive scattering of atomic oxygen from Si(100) is found. This suggests that the rate-limiting step in void growth is oxide decomposition at the void perimeter to produce SiO(*g*).

Due to its technological importance, the Si/SiO<sub>2</sub> interface has been investigated extensively.<sup>1</sup> In particular, the decomposition of thick SiO<sub>2</sub> films has been studied in some detail in order to better understand failure in silicon field effect transistors. It has been demonstrated that the thermal decomposition of uniform SiO<sub>2</sub> films of a few hundred angstroms thickness grown on a Si(100) substrate proceeds inhomogeneously. Decomposition occurs with the formation of approximately circular voids which expose the clean substrate. The voids grow laterally in time at constant temperature and the oxide film between the voids appears to be unchanged until it is engulfed by the growing voids.<sup>2,3</sup>

It would be of interest to see whether the decomposition of films of a few angstroms thickness, whose composition will not be SiO<sub>2</sub> as for thick films, also proceeds inhomogeneously. This would allow a more detailed mechanistic study of the reaction since a variety of standard surface science techniques could be utilized. We report here the results of such studies in which the oxide film was produced by the adsorption of atomic oxygen on a Si(100) substrate. Our results concerning the decomposition kinetics of films whose thickness is in the range of zero to four monolayers (ML) will be presented elsewhere.<sup>4</sup> We focus here on studies of spatial inhomogeneity with detailed results for an initial oxygen coverages between 4 and 10 ML.

The experiments were carried out in a molecular-beam apparatus which has been described elsewhere.<sup>5</sup> Briefly, it consists of a UHV scattering chamber with a three stage differentially pumped beam line. X-ray photoelectron spectroscopy (XPS), ion scattering spectroscopy (ISS), and modulated beam mass spectrometric studies can be carried out. The *n*-type Si(100) sample has the form of a 1 × 3 cm<sup>2</sup> rectangle and has a resistivity of 16–24 Ω cm. It is mounted at the intersection of the atomic beam, the x-ray source, the hemispherical energy analyzer lens axis, and the ion gun. The mass spectrometer, which was differentially pumped with liquid-nitrogen-cooled copper shrouds, was mounted in line of sight to the sample. The Si(100) surface was cleaned by cycles of argon-ion sputtering and heating to 1270 K. Elevated temperatures were achieved by a combination of radiative and resistive

heating and controlled by optical pyrometer detection (above 900 K) coupled with an optimal feedback method.<sup>6</sup> The atomic oxygen beam was formed by supersonic expansion of a rf-induced plasma in a 5% O<sub>2</sub>-He mixture and had a mean translational energy of 16 kcal/mol.<sup>7</sup> Absolute oxygen coverages were determined by XPS using the oxygen peak from adsorbed water as a calibration.<sup>8,9</sup> Extremely reproducible doses could be obtained using a computer controlled beam valve. Adsorption was carried out at 900 K and the heating rate in thermal-desorption experiments was 6.0 Ks<sup>-1</sup> unless otherwise indicated. The sample temperature was cooled to 900 K after each thermal-desorption experiment at a rate of ~3 Ks<sup>-1</sup> in order to anneal the surface well.

The only gas-phase decomposition product of the oxide film which we observe is SiO, in agreement with earlier studies.<sup>5</sup> The peak temperature for SiO(*g*) in a thermal-desorption experiment increases dramatically with increasing initial oxygen coverage up to 16 ML.<sup>7</sup> At this point it is essential to make a distinction between the local and the average coverage. The average coverage measured with XPS or by integrating the signal in a thermal-desorption experiment is a valid concept when the adsorbate is uniformly distributed. However, if this is not the case, only the local coverage is meaningful. Variations in the local coverage might arise, for instance, through inhomogeneous partial desorption. For this particular system, the local coverage can be measured using the dependence of the thermal-desorption peak temperature on the initial coverage. Since our experiments have shown that the desorption peak temperature is a unique function of the local coverage, readsorption of oxygen following partial desorption can be used to probe the mode of decomposition. We illustrate these statements by the following example. Partial isothermal desorption at 1090 K followed by cooling to 900 K and a subsequent thermal-desorption experiment show that the peak temperature is essentially unchanged (1170–1150 K), as the average coverage is decreased from 4.50 ML to 0.82 ML. The corresponding peak temperatures for initial coverages of 4.50 and 0.82 ML are 1170 and 980 K, respectively.

Consider readsorption on these surfaces generated by partial desorption from an initial coverage of 4.50 ML. If

the desorption occurs homogeneously, subsequent readsorption will result in a single peak characteristic of the coverage following readsorption. If decomposition occurs inhomogeneously with voids exposing the clean silicon substrate in an oxide of unchanged local coverage, two peaks will be observed in a thermal-desorption experiment. One would be characteristic of the coverage in the voids following readsorption and the other would be characteristic of the initial coverage, since for the small readsorption doses used, further adsorption on the oxide film can be neglected. The upper part of Fig. 1 illustrates that inhomogeneous decomposition is taking place on the surface. It is seen that thermal desorption with or without readsorption leads to an identical high-temperature peak. However, readsorption gives rise to a second peak at a lower temperature. Exposing a clean surface to the same dose used in readsorption gives rise only to a low-temperature peak which has the same shape and peak temperature as that obtained after readsorption. They differ only in the area under the curves which is proportional to the average coverage. This is greater for adsorption on the clean crystal than for readsorption.

The lower part of Fig. 1 shows a summary of experiments with increasing isothermal desorption prior to readsorption. The negligible shift of the high-temperature peak indicates that the local coverage in the oxygen

covered parts of the surface are unchanged from the initial value of 4.50 ML. The presence of a second low-temperature peak is consistent with inhomogeneous decomposition. Two important points should be made concerning the low-temperature peak. It occurs at the same temperature and has the same shape independent of the degree of desorption in the isothermal phase up to complete desorption. Therefore the peak is characteristic of adsorption on the clean Si(100) substrate. These observations indicate that during inhomogeneous desorption voids exposing clean substrate are formed and that there is no oxygen depletion outside of the void area.

The information contained in the lower part of Fig. 1 also allows a determination of the fractional surface area of the voids  $\theta_{\text{void}}$  to be made. The integrated low-temperature thermal desorption signal  $A_r$  following a fixed readsorption dose after partial desorption is smaller than that for the same dose on a clean surface  $A_r^0$ . The reason for this is that readsorption takes place only on the total void area exposed which is only a fraction  $\theta_{\text{void}}$  of the clean surface area. Therefore the ratio of the integrated thermal desorption signal after readsorption following partial desorption to that measured on a clean surface is given by

$$\theta_{\text{void}} = \frac{A_r}{A_r^0} = \frac{A_{\text{void}}}{A_{\text{surface}}}, \quad (1)$$

where  $A_{\text{surface}}$  and  $A_{\text{void}}$  indicate the total area of the clean substrate and void area exposed to the beam, respectively.

To test whether the lack of a shift in the peak temperature of the high-temperature peak in the lower part of Fig. 1 is conclusive evidence for the absence of a change in local coverage of the oxide covered part of the surface during the isothermal desorption, we analyzed the data resulting from readsorption of oxygen on silicon oxide films generated by partial desorption in a second way. If the oxide film between voids remains intact,

$$\theta_{\text{void}} = 1 - \frac{\theta_{\text{ox}}}{\theta_{\text{ox}}^0} = 1 - \frac{A}{A_i}, \quad (2)$$

where  $\theta_{\text{ox}}$  and  $\theta_{\text{ox}}^0$  are the oxygen coverages after and prior to partial desorption and  $A$  and  $A_i$  are the integrated thermal desorption signals after and without partial desorption, respectively. As the plot in Fig. 2 shows, the experimentally determined void area  $\theta_{\text{void}}$  can be described very well by Eq. (2). Both sets of experiments described above verify that desorption occurs inhomogeneously through void formation. Furthermore, our experiments show that the oxygen coverage in the voids is zero and that the oxide between the voids does not change in coverage as the voids increase in area.

Our measurements clearly establish that decomposition occurs through void formation, but give neither information on the size of individual voids or where on the surface they nucleate. Previous studies on thick films measured only diameters larger than 10  $\mu\text{m}$  (Refs. 2 and 3) which gives no information on the atomic scale. Very recent scanning tunneling microscope (STM) have provided microscopic information. Partial desorption from 12-Å thick oxide films was carried out in vacuum after which STM

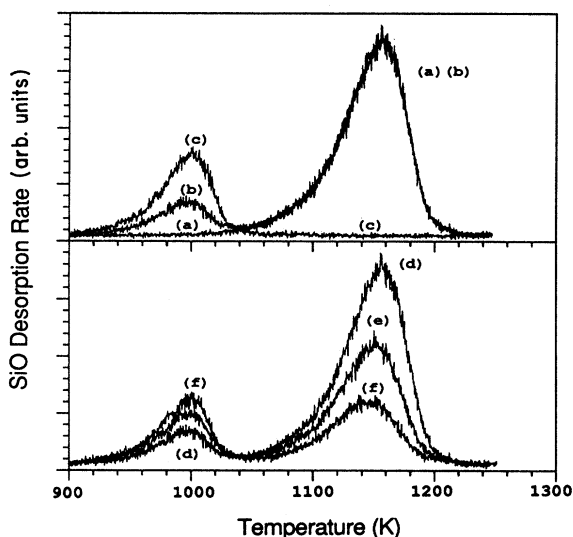


FIG. 1. Curve *a*, thermal-desorption spectrum of SiO(*g*) for an initial coverage of 4.50 ML generated by a 120 s exposure to the atomic oxygen beam at 900 K. Partial isothermal desorption has been carried out at 1090 K for 50 s to reduce the coverage to 2.38 ML. Curve *b*, same as for curve *a*, except that the sample has been exposed to the atomic oxygen beam for an additional 2.2 s at 900 K prior to temperature programmed desorption. Curve *c*, thermal-desorption spectrum following exposure of the clean sample at 900 K to the atomic oxygen beam for 2.2 s. Curves *d* to *f* are thermal-desorption spectra of SiO(*g*) following isothermal desorption from an initial coverage of 4.50 ML by heating at 1090 K for curves *d* 50, *e* 76, and *f* 105 s and subsequent exposure of the resulting surface to the atomic oxygen beam for 2.2 s at 900 K.

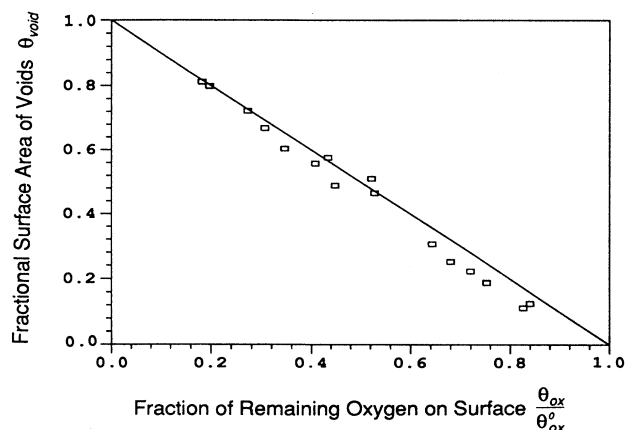


FIG. 2. Plot of  $\theta_{\text{void}}$  vs  $(1 - A/A_i)$ .

analysis was carried out after exposure to the air.<sup>10</sup> Approximately circular voids down to  $\sim 1000$  Å in diameter were resolved. It was seen that as desorption proceeds, the void diameter increased, but the number of voids remains approximately constant. Whereas previous studies image voids directly on all significant length scales, the mechanism for the decomposition has not been clearly established. For this reason we have undertaken kinetic studies of the void growth in the oxide film.

We have carried out measurement using both isothermal techniques and temperature programmed desorption in which the temperature was increased linearly with time. We begin with a kinetic model which describes desorption with void formation. To simplify the model, let us consider that all voids are circular and have the same radius  $r$ , and that they occur with a constant density of  $n_{\text{void}}$  per  $\text{cm}^2$ . We assume that SiO can only be produced

at the void perimeter, so that

$$-\frac{d(\theta_{\text{ox}}n_{\text{ox}})}{dt} = n_{\text{void}}k_r2\pi r\rho\theta_{\text{ox}}^0, \quad (3)$$

where  $\theta_{\text{ox}}$  is the average coverage of oxygen,  $n_{\text{ox}}$  is the site density on the Si(100) plane ( $6 \times 10^{14} \text{ cm}^{-2}$ ),  $\rho$  is the line density of oxygen atoms on the void perimeter, and  $k_r$  is the rate constant which we assume to have the form  $k_r = \nu_r \exp -E_r/k_B T$ , and  $\theta_{\text{ox}}^0$  is the initial oxide coverage. Substituting the expression  $\theta_{\text{ox}} = (1 - n_{\text{void}}\pi r^2)\theta_{\text{ox}}^0$  into Eq. (3), and setting  $\rho^2 = n_{\text{ox}}$  we obtain at a constant temperature

$$r(t) = k_r/(n_{\text{ox}})^{1/2}t, \quad (4)$$

and

$$-\frac{d\theta_{\text{ox}}}{dt} = \left[ \frac{2\pi n_{\text{void}}k_r^2\theta_{\text{ox}}^0}{n_{\text{ox}}} \right] t. \quad (5)$$

Equations (4) and (5) predict that for isothermal desorption both the void diameter and the desorption rate of SiO increase linearly with time. As can be seen in Fig. 3, this model holds for the initial stage of desorption. The decrease in rate after the maximum can be attributed to the overlap of voids which leads to a decrease in the perimeter at which the reaction occurs. This occurs when approximately 40% of the film has been desorbed. The slope of the initial linear portion should be strongly temperature dependent since it is proportional to  $k_r^2$ . By plotting the logarithm of the slope as a function of the reciprocal temperature, a straight line would result with a slope of  $-2E_r/k_B$  and an intercept of  $\log 2\pi n_{\text{void}}k_r^2\theta_{\text{ox}}^0/n_{\text{ox}}$ . This is indeed the case, as shown in the inset of Fig. 3, over the limited temperature range accessible in our experiment. The activation energy of SiO(g) production is determined to be for  $\sim 94$  ( $\sim 87$ ) kcal/mol for  $\theta_{\text{ox}}^0 = 10.5$  (7.0) ML.

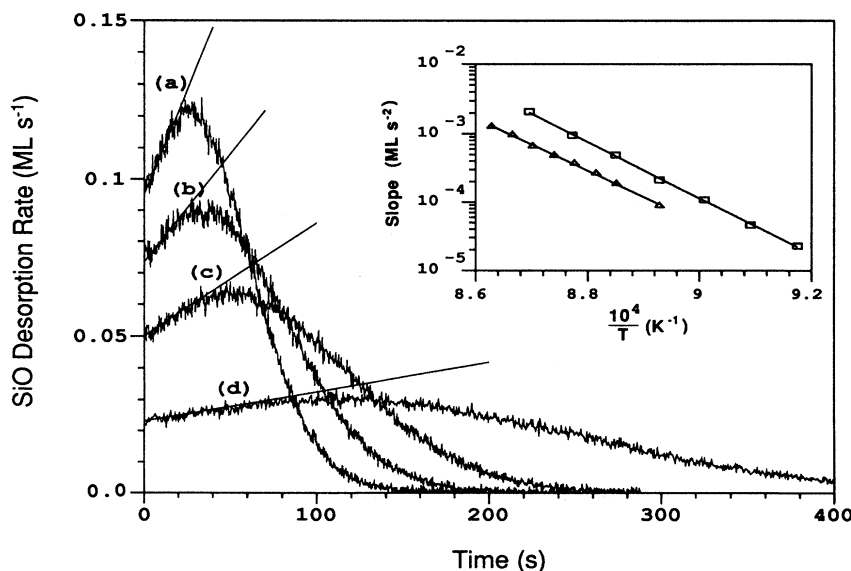


FIG. 3. Isothermal rate of SiO desorption as a function of time for temperatures of curves *a*, 1159 K; *b*, 1149 K; *c*, 1140 K; and *d*, 1120 K. The initial coverage was 10.5 ML. Inset: Slope of the initial linear portion in the figure as a function of reciprocal temperature for initial coverages ( $\square$ ) 7.0 ML and ( $\triangle$ ) 10.5 ML.

From the intercept, the value of  $(n_{\text{void}})^{1/2}v_r$  is determined to be  $9.6 \times 10^{22}$  ( $4.7 \times 10^{21}$ )  $\text{s}^{-1}\text{cm}^{-1}$  for  $\theta_{\text{ox}}^0 = 10.5$  ML and (7.0) ML, respectively. In view of the limited number of experiments we have carried out and the small temperature range over which data could be collected, we do not consider the differences reported here at these two coverages to be significant.

To determine the value of the preexponential factor, the void density must be known. If we assume that our sample has the same void density of  $10^9 \text{cm}^{-2}$  that was determined in recent STM experiments for a Si(100) sample,<sup>10</sup> we obtain preexponential values of  $3 \times 10^{18} \text{s}^{-1}$  and  $2 \times 10^{17} \text{s}^{-1}$  for  $\theta_{\text{ox}}^0 = 10.5$  and 7.0 ML, respectively. This is in the range of what could be expected on the basis of transition state theory. With these values,  $dr(t)/dt = 1.5 \text{\AA s}^{-1}$  and  $1.7 \text{\AA s}^{-1}$  at 1090 K for initial coverages of 10.5 and 7.0 ML, respectively. The similarity of the activation energy determined here to the value determined by scattering an oxygen atom from a high-temperature Si(100) surface to produce SiO (80 kcal/mol) (Refs. 7 and 11) suggests that the energetics are the same for the activated complexes involved. In view of the assumption which must be made concerning the void density to extract a value for the preexponential factor, it is difficult to assess whether the difference between the value determined in Ref. 11 ( $10^{19} \text{s}^{-1}$ ) and that determined here is real.

It is of interest to compare the relative ability of isothermal and temperature programmed methods to yield mechanistic information and precise values for the kinetic parameters. Temperature programmed desorption (TPD) experiments were carried out using a fixed initial coverage of 7.0 ML and varying the heating rate between 0.1 and 6  $\text{K s}^{-1}$ . From the collected data set,  $E_r(\theta)$  and  $f(\theta)/\theta$  in the generalized rate expression

$$-\frac{d\theta_{\text{ox}}}{dt} = f(\theta)\exp[-E_r(\theta)/k_B T]$$

can be determined.<sup>12</sup> They vary only slowly with coverage and have values near 90 kcal/mol and  $10^{15}$ – $10^{16} \text{s}^{-1}$ , respectively. Since  $f(\theta)/\theta$  has the value generally expected for a homogeneous first-order surface reaction, distinguishing between this and the inhomogeneous reaction mechanism verified above is not possible using the TPD data alone. Whereas the isothermal studies are more useful in determining the reaction mechanism, the TPD results give a higher precision for  $E_r(\theta)$ . The isothermal data can only be analyzed by assuming that  $E_r$  is independent of coverage and the temperature range over which the experiment can be carried out is too small to allow an accurate measurement. For these reasons, a combination of both measurements is well suited to a mechanistic study as well as a quantitative determination of the kinetic parameters.

<sup>1</sup>*SiO<sub>2</sub> and its Interfaces*, edited by S. T. Pantelides and G. Lucovsky, MRS Symposia Proceedings No. 105 (Materials Research Society, Pittsburgh, 1988).

<sup>2</sup>M. Liehr, J. E. Lewis, and G. W. Rubloff, *J. Vac. Sci. Technol. A* **5**, 1559 (1987).

<sup>3</sup>G. W. Rubloff, *J. Vac. Sci. Technol. A* **8**, 1853 (1990).

<sup>4</sup>Y.-K. Sun, D. Bonser, and T. Engel (unpublished).

<sup>5</sup>M. P. D'Evelyn, M. M. Nelson, and T. Engel, *Surf. Sci.* **186**, 75 (1987).

<sup>6</sup>J. R. Engstrom and W. H. Weinberg, *Rev. Sci. Instrum.* **55**, 404 (1984).

<sup>7</sup>J. R. Engstrom, D. J. Bonser, M. M. Nelson, and T. Engel, *Surf. Sci.* (to be published).

<sup>8</sup>D. Schmeisser, *Surf. Sci.* **137**, 197 (1984).

<sup>9</sup>W. Ranke and Y. R. Xing, *Surf. Sci.* **157**, 339 (1985).

<sup>10</sup>Y. Kobayashi and K. Sugii (unpublished).

<sup>11</sup>J. R. Engstrom and T. Engel, *Phys. Rev. B* **41**, 1038 (1990).

<sup>12</sup>J. L. Taylor and W. H. Weinberg, *Surf. Sci.* **78**, 259 (1978).